JPE 15-6-1

http://dx.doi.org/10.6113/JPE.2015.15.6.1421
ISSN(Print): 1598-2092 / ISSN(Online): 2093-4718

Modified Dual-Buck Inverter Based on Resonant Link

Rong Chen†, Jia-Sheng Zhang*, and Wei Liu*

†,*College of Information and Control Engineering, China University of Petroleum (Huadong), Qingdao, China

Abstract

The efficiency and reliability of the dual-buck inverter (DBI) were greatly improved by eliminating the shoot-through problem and optimally designing the freewheeling diode. The traditional DBI suffers from large harmonic components with low output voltage and large capacity output filter inductor. To overcome the aforementioned disadvantages, a modified DBI (MBDI) was proposed by adopting a quasi-resonant link and pulse density modulation (PDM). This paper first introduces the working principle of the MBDI and PDM, and then the selection principle of system parameters is presented. Finally, a mathematical model of the MBDIis built, and an experiment prototype is set up. Simulation and experimental results verify the correctness of the theoretical analysis and the feasibility of the scheme.

Key Words: Dual-buck inverter, Pulse density modulation, Quasi-resonant link, Three-level hysteresis controller

I. INTRODUCTION

With the development of power devices and the advancement of inverter topology, the high-performance voltage source inverter (VSI) has generated wide research appeal [1], [2]. The conventional bridge-type VSI is widely used. However, it suffers from the shoot-through problem and the long reverse recovery time of the body diode. The shoot-through problem greatly limits the reliability of the inverter. The dead time, which results in the output voltage distortion and affects the quality of the output of the inverter, has to be provided in the VSI to block the upper and lower switching devices of each leg of a bridge [3], [4]. The long reverse recovery time of the body diode and large loss also affect the reliability and efficiency of the inverter, particularly the medium frequency inverter [5], [6]. Therefore, to achieve higher performance, more works focus on the DC/AC inverter based on the DC/DC converter.

Thus, a highly reliable dual-buck inverter (DBI) should be developed [7]. The DBIis composed of two buck converters, and one switching device of each leg of the bridge is replaced by an independent freewheeling diode. For the DBI, only one switch device works at any time, thereby improving the reliability of the inverter. The shoot-through problem is overcome by an in-series filter inductor between two switching devices, which leads to greatly enhanced reliability [8], [9]. The DBIis not limited by the dead time issues of the conventional VSI, which can easily push the duty cycle to the theoretical limit and fully transfer the energy to the load through total pulse width modulation (PWM) because of the lack of the shoot-through problem [10]-[13]. The freewheeling current flows through the independent freewheeling diodes instead of the body diode of the switching device, which induces large loss and limits the switching frequency of inverter; thus, the freewheeling diode can be designed optimally. The fast recovery diode and the silicon carbide diode are used as independent freewheeling diodes [14].

Various control strategies used on the DBI have been proposed. Voltage single closed-loop control for DBI was proposed. Adopting the single closed-loop control is a better method to keep the dynamic characteristic and stability of the DBI. However, the single closed-loop control cannot achieve direct control of average current flowing through the filter inductor, which leads to the output voltage distortion. The voltage–current double closed-loop control, which originated from speed-current double closed-loop control system, has also been proposed [15]. The addition of inner current loop can greatly speed up the process of resisting load disturbance. In

Manuscript received Dec. 2, 2014; accepted May 14, 2015
Recommended for publication by Associate Editor Joung-Hu Park.
†CorrespondingAuthor:chenrongjn@163.com
Tel: +86-153-7690-9720,Fax: +86-532-83154820, China University of Petroleum (Huadong)
*College of Information and Control Engineering, China University of Petroleum (Huadong), China

this condition, the control strategy used on the DBI has been developed continuously. However, the DBI suffers from large harmonic components with low output voltage when the input voltage is high and large capacity output filter inductor, which is not conducive to the miniaturization of the system.

A modified DBI (MDBI) is proposed in this paper. The front-end quasi-resonant link is introduced to reduce harmonic components with low output voltage. The pulse density modulation (PDM) is used, which can decrease the value of the filter inductor and reduce the size of the inverter. The MDBI works in voltage–current double closed-loop mode and is controlled by the three-level hysteresis controller. The working principle of the MDBI is described in Section II, whereas the parameter selection principle is illustrated in Section III.A mathematical model and simulation results are presented in Section IV, and Section V presents the results from an experiment prototype. Finally, the concluding remarks are given in Section VI.

II. WORKING PRINCIPLE OF THE MODIFIED DUAL-BUCK INVERTER

Fig. 1 shows the schematic of the MDBI. It consists of the positive soft-switching resonant circuit and the negative soft-switching resonant circuit [16]. The positive soft-switching resonant circuit is composed of L_1, S_1, C_1, S_2, L_2, and C_o. The negative soft-switching resonant circuit constitute is comprised of L_3, S_3, C_2, S_4, L_4 and C_o.

To commence with the analysis, some conditions are assumed as follows.

1) All the switches and diodes are ideal.

2) All the inductors and capacitors are ideal.

3) The output voltage (u_o) and the reference voltage (u_{ref}) are constant in one switching cycle.

4) The resonant frequency is much higher than the frequency of output voltage.

5) L_1=L_2=L_3=L_4 and C_1=C_2.

The MDBI is controlled by a three-level hysteresis controller to obtain a good sinusoidal output voltage. To obtain a sinusoidal output voltage, a sinusoidal reference is required. Reference signal v_{ref} is shown in Fig. 2(a). To force the output voltage to track u_{ref}, upper limit u_U and lower limit u_L, are generated from u_{ref}. These three signals are used to form the hysteresis band.

During the construction of the positive half cycle of the output voltage, signals u_{ref} and u_U form the band within which the output should remain. The working principle of the positive soft-switching resonant circuit during a comparison process is shown in Fig. 2(b). If the output voltage is below u_{ref}, the positive soft-switching resonant circuit will work and remain until the output voltage enters the band. Once that happens, the positive soft-switching resonant circuit will stop output

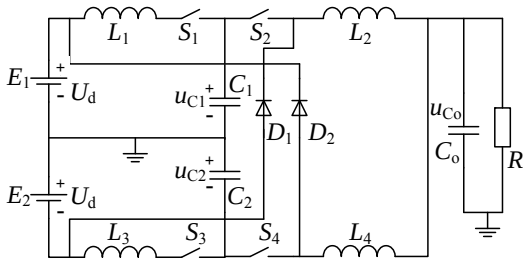

Fig. 1. Schematic of the MDBI.

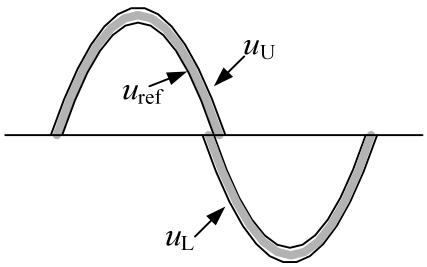

(a) Reference signal v_{ref} and output voltage.

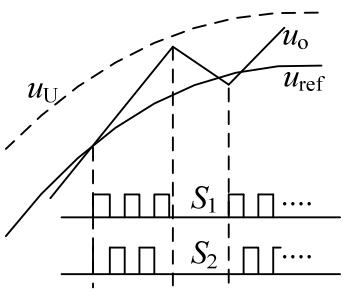

(b) Working principle of the positive soft-switching resonant circuit during a comparison process.

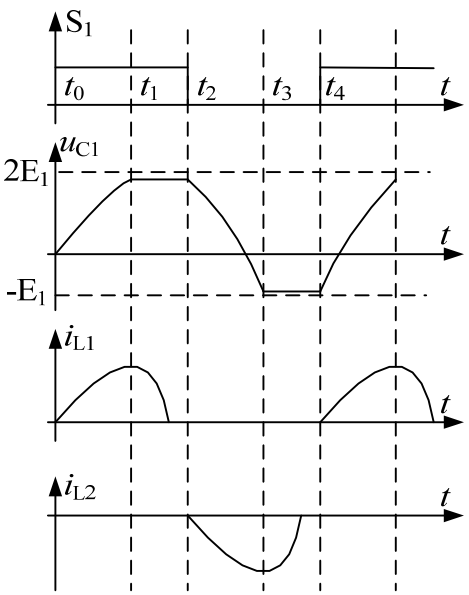

(c)i_{L1},i_{L2}, and u_{C1} during a few switching periods.

Fig. 2. Working principle of the MDBI.

working and the energy is transferred from $E_1$to the load and capacitor. To restrict such an increment in the output voltage, upper band u_U is used. As long as the output voltage lies within the band formed by u_{ref} and u_U, the positive soft-switching resonant circuit will stop working, and a corrective action follows only after the output voltage has moved out of the band. If the output voltage goes beyond u_U, the negative soft-switching resonant circuit will work until the output voltage reenters the band. If the output voltage falls below u_{ref}, the positive soft-switching resonant circuit is activated until the output voltage reenters the band. During the negative half cycle of the output voltage, the control band is formed by u_{ref} and u_L and followed by a similar logic.

The working time of the positive soft-switching resonant circuit is determined by the hysteresis bands. During the working time, the positive soft-switching resonant circuit works as follows. The current through inductors L_1 and L_2 and the voltage across capacitor C_1 during a few switching periods are depicted in Fig. 2(c).

(1) Stage 1 [t_0,t_1]:At t=t_0, switch $S_1$is turned on, and S_2 is turned off. The zero-current resonant circuit is composed of L_1, C_1, andS_1.Energy from E_1 is transferred to resonant capacitor C_1.At t=t_1, the voltage across resonant capacitor C_1, u_{C1}, reaches maximum, u_{c1max}≈2U_d. Switch S_1 is turned off with zero-current switching (ZCS) because of resonant inductor L_1. The energy stored in output capacitor C_o is transferred to load.

(2)Stage 2 [t_1, t_2]:SwitchesS_1 and S_2 are turned off. The energy stored in output capacitor C_o is transferred to the load.

(3) Stage3 [t_2, t_3]: At t=t_2, switch $S_1$is turned off, and S_2 is turned on. The zero-current resonant circuit is composed of L_2, C_o,C_1, and S_2. C_o is equivalent to the constant voltage source because C_o>>C_1. The energy stored in resonant capacitor C_1 is transferred to the load and output capacitor C_o. Because of resonant inductor L_2, at t=t_3, the voltage across resonant capacitor reaches the minimum, u_{c1min} ≈ U_{Co}, and S_2 is turned off with ZCS.

(4) Stage 4 [t_3, t_4]:SwitchesS_1 and $S_2$are turned off. The energy stored in output capacitor C_o is transferred to the load. This stage ends at t=t_4, when switch S_1 is turned on to start the next operation cycle.

The positive soft-switching resonant circuit will work repeatedly until the desired voltage is obtained. The period T=t_4-t_0 is the working cycle of the pulse, which is used to realize the ZCS.

The previous analysis shows that the energy transferred from E_1 to output capacitor C_o, and the load can be changed by adjusting the pulse density, which is called the PDM.

III. PARAMETER SELECTION OF THE MODIFIED DUAL-BUCK INVERTER

The selection of the resonant inductor and resonant capacitor plays an important role in the ability to transfer energy from E_1or E_2 to the load by resonant circuit. Assuming L = L_1 = L_2 = L_3 = L_4 and C = C_1 = C_2<< C_o, the resonant frequency f and the period T are

$$f = \frac{1}{2\pi\sqrt{LC}} \tag{1}$$

and

$$T = 2\pi\sqrt{LC}\,. \tag{2}$$

Because of the maximum voltage across resonant C_1 and C_2 is $2U_d$, the maximum energy stored in the resonant capacitor during one cycle may be calculated as

$$\frac{1}{2}CU_{c1\max}^2 = 2CU_d^2\cdot \tag{3}$$

The amount of energy transferred from E_1 or E_2 to the load within a unit time is

$$W = 2CU_d^2 \times f = \frac{U_d^2}{\pi}\sqrt{\frac{C}{L}}\,. \tag{4}$$

Equation (4) shows that the amount of energy transferred is proportional to resonant capacitor C_1/C_2 and resonant frequency f. If resonant frequency f is constant, the greater the capacitor, the more energy is transferred. However, the greater the capacitor, the smaller the resonant inductor, which results in the instantaneous current flowing in the resonant capacitor to become too large, and the normal operation of inverter is affected.

The resonant frequency of the series-resonant circuit, which is composed of C_1, S_2, L_2, and C_o, is

$$f = \frac{1}{2\pi\sqrt{L_2\dfrac{C_1C_o}{C_1+C_o}}}\quad . \tag{5}$$

Because C=C_1=C_2<<C_o, Equation (1) is used in practical applications. Resonant inductors L=L_1=L_2=L_3=L_4=40μH and resonant capacitors C=C_1=C_2=0.15μH are used.

The output capacitor is used to filter out high-order harmonic component of output voltage u_{Co}. The greater the output capacitor, the better the filter. However, if the output voltage is constant, the greater the output capacitor C_o, the larger the reactive-current flowing in the output capacitor, which increases the size and weight of the inverter and reduces efficiency of the inverter. In general, the current flowing in the output capacitor is less than 50% I_o. Output power is 160VA. Output voltage is 48V. Output current is given as

$$I_o = \frac{P_o}{U_o} = \frac{160}{48} = 3.33A\cdot \tag{6}$$

The current flowing in the output capacitor is I_{Co}≤1.67A.

The current flowing in the output capacitor can be defined as

$$I_{Co} = C_o\frac{dU_o}{dt}\,. \tag{7}$$

According to Equation (7), the output capacitor can be calculated as

$$C_o \le \frac{I_{Co}}{U_o\omega} = \frac{1.67}{48\times 50\times 2\pi} = 110\mu\text{F} \tag{8}$$

where C_o=60μF is used.

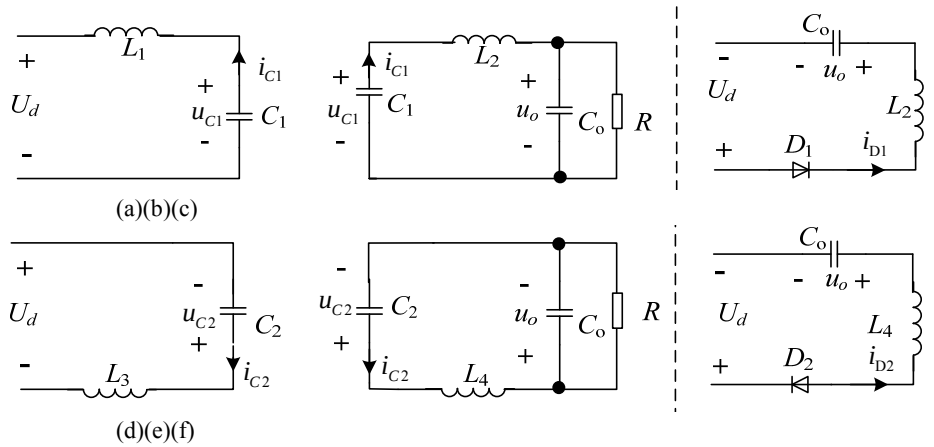

Fig. 3. Effective working status of MDBI.

IV. Mathematical Model and Simulation Results of Modified Dual-Buck Inverter

Because the resonant period of the quasi-resonant circuit is equal to or less than the switching period, which does not comply with linear assumption of harmonic components, the traditional state-space method is no longer applicable. Symbolic analysis [17] and discrete mapping modeling [18] are used, and a mathematical model of the MDBI is proposed.

Seven state variables exist, i.e.,u_{C1}, i_{C1}, u_{Co}, u_{C2}, i_{C2}, i_{D1}, and i_{D2}.Referencesignal $u_{ref} = 48\sqrt{2}\sin(100\pi * t)$. The effective working status of the MDBI is shown in Fig.3.The differential equation of Fig.3 can be obtained as follows:

Table I shows the symbolic functions.

$$
(a)\begin{cases} \dfrac{du_{C1}}{dt} = -\dfrac{1}{C_1} i_{C1} \\ \dfrac{di_{C1}}{dt} = \dfrac{-U_d + u_{C1}}{L_1} \\ \dfrac{du_o}{dt} = 0 \end{cases}
\quad
(b)\begin{cases} \dfrac{du_{C1}}{dt} = -\dfrac{1}{C_1} i_{C1} \\ \dfrac{di_{C1}}{dt} = \dfrac{-u_o + u_{C1}}{L_2} \\ \dfrac{du_o}{dt} = \dfrac{i_{C1}}{C_o} \end{cases}
\quad
(c)\begin{cases} \dfrac{du_o}{dt} = \dfrac{i_{D1}}{dt} \\ \dfrac{di_{D1}}{dt} = \dfrac{-U_d - u_o}{L_2} \end{cases}
$$

$$
(d)\begin{cases} \dfrac{du_{C2}}{dt} = -\dfrac{1}{C_2} i_{C2} \\ \dfrac{di_{C2}}{dt} = \dfrac{U_d + u_{C2}}{L_3} \\ \dfrac{du_o}{dt} = 0 \end{cases}
\quad
(e)\begin{cases} \dfrac{du_{C2}}{dt} = -\dfrac{1}{C_2} i_{C2} \\ \dfrac{di_{C2}}{dt} = \dfrac{U_d + u_{C2}}{L_3} \\ \dfrac{du_o}{dt} = 0 \end{cases}
\quad
(f)\begin{cases} \dfrac{du_o}{dt} = \dfrac{i_{D2}}{C_o} \\ \dfrac{di_{D2}}{dt} = \dfrac{U_d - u_o}{L_4} \end{cases}
\tag{9}
$$

$$
\begin{bmatrix} \dot{u}_{C1} \\ \dot{u}_{C2} \\ \dot{i}_{C1} \\ \dot{i}_{C2} \\ \dot{u}_o \\ \dot{i}_{D1} \\ \dot{i}_{D2} \end{bmatrix}
=
\begin{bmatrix}
0 & 0 & -\dfrac{s_1+s_2}{C_1} & 0 & 0 & 0 & 0 \\
0 & 0 & 0 & -\dfrac{s_3+s_4}{C_1} & 0 & 0 & 0 \\
\dfrac{s_1}{L_1}+\dfrac{s_2}{L_3} & 0 & 0 & 0 & -\dfrac{s_2}{L_3} & 0 & 0 \\
0 & \dfrac{s_3}{L_1}+\dfrac{s_4}{L_3} & 0 & 0 & -\dfrac{s_4}{L_3} & 0 & 0 \\
0 & 0 & \dfrac{s_2}{C_o} & \dfrac{s_4}{C_o} & -\dfrac{1}{C_o R} & \dfrac{s_5}{C_o} & \dfrac{s_6}{C_o} \\
0 & 0 & 0 & 0 & -\dfrac{s_5}{L_3} & 0 & 0 \\
0 & 0 & 0 & 0 & -\dfrac{s_6}{L_4} & 0 & 0
\end{bmatrix}
\begin{bmatrix} u_{C1} \\ u_{C2} \\ i_{C1} \\ i_{C2} \\ u_o \\ i_{D1} \\ i_{D2} \end{bmatrix}
+
\begin{bmatrix}
0 & 0 \\
0 & 0 \\
-\dfrac{s_1}{L_1} & 0 \\
0 & \dfrac{s_3}{L_1} \\
0 & 0 \\
0 & -\dfrac{s_5}{L_3} \\
\dfrac{s_6}{L_4} & 0
\end{bmatrix}
\begin{bmatrix} U_d \\ U_d \end{bmatrix}
\tag{10}
$$

TABLE I
SYMBOLIC FUNCTION

$u_{ref}>u_o$

time	S_1	S_2	S_3	S_4	S_5	S_6
t_0-t_1	1	0	0	0	0	0
t_1-t_2	0	0	0	0	0	0
t_2-t_3	0	1	0	0	0	0
t_3-t_4	0	0	0	0	1	0

$u_{ref}<u_o$

time	S_1	S_2	S_3	S_4	S_5	S_6
t_0-t_1	0	0	1	0	0	0
t_1-t_2	0	0	0	0	0	0
t_2-t_3	0	0	0	1	0	0
t_3-t_4	0	0	0	0	0	1

Combing the state equation with the symbolic function gives a comprehensive estate function equation, as shown in equation (10).

The state equation of MDBI can be set as

$$\dot{x} = Ax + Bu. \tag{11}$$

The state variable x(t) is

$$x(t) = \Phi(t)x_0 + \int_0^{\tau} \Phi(t-\tau)Bu(\tau)d\tau \tag{12}$$

where

$$\Phi(t) = e^{At} = I + At + \frac{1}{2!}A^2t^2 + \cdots + \frac{1}{n!}A^nt^n + \cdots \tag{13}$$

Supposing the input is constant, a discrete iteration equation may be derived:

$$x_{n+1} = \Phi(kH)x_n + \Phi_m(kH)U \tag{14}$$

where H is sample time and

$$\begin{cases} \Phi(H) = e^{AHk} \\ \Phi_m(H) = \int_0^{kH} e^{A(kH-\tau)}Bd\tau = \int_0^{kH} \Phi(kH-\tau)Bd\tau \end{cases} \tag{15}$$

Equation (15) can be solved by iteration, and simulation results are shown in Fig.4.As shown in Fig. 4(a), output voltage u_o can track reference signal u_{ref}. Fig. 4(b) shows the voltage across resonant capacitor C_1u_{C1}, which validates that maximum voltage u_{C1max} is close to $2U_d$. Fig. 4(c) shows the driving signals of S_1 and S_2. As shown in Fig. 4(c),the working time of the negative soft-switching resonant circuit is longer than the positive soft-switching resonant circuit when $u_{ref}<0$ and vice versa.

V. EXPERIMENT RESULTS

To verify the results from the simulation and test the usefulness of the MDBI, a 160-VA prototype is fabricated in the laboratory. The parameter of the MDBI is listed in Table II.

The experiment results are shown in Fig. 5. Fig. 5(a) depicts the output voltage of the DBI and the MDBI, which shows that the harmonic components of the DBI is much higher than that of the MDBI. When the output filter inductor and output

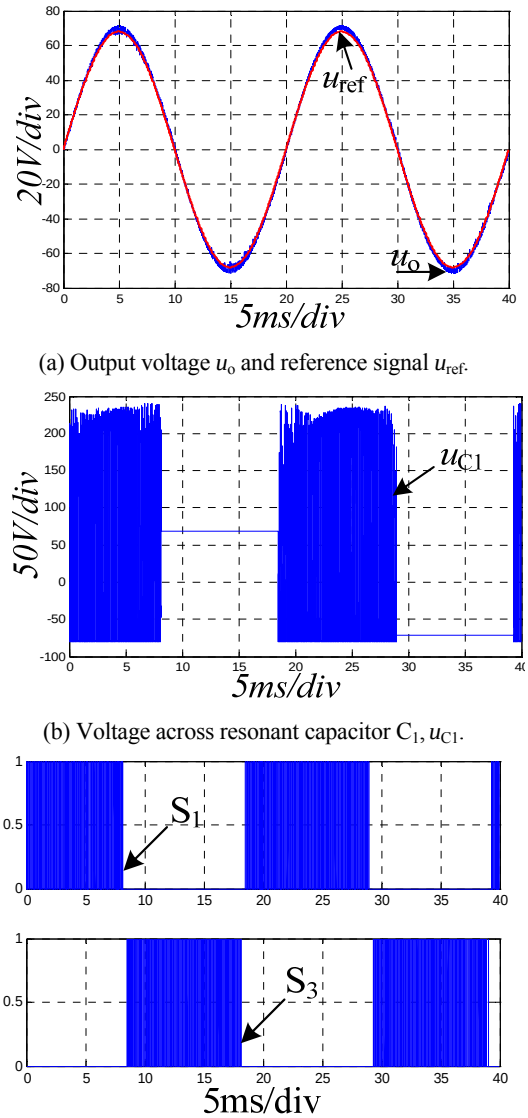

(a) Output voltage u_o and reference signal u_{ref}.

(b) Voltage across resonant capacitor C_1, u_{C1}.

(c) Driving signals of S_1 and S_2.

Fig. 4. Simulation results of the MDBI.

TABLE II
THE PARAMETER OF THE MDBI

Parameter	Value
input voltageU_d/V	110
output frequencyf_o/Hz	50
output capacitorC_o/iF	60
resonant capacitor C_1 , C_2/iF	0.15
L_1, L_2, L_3, L_4/μH	40
resonant frequency/kHz	30

capacitor for the DBI and the MDBI are identical, C_o=60iF and L_2=L_4=40μH,and the harmonic components of the DBI and the MDBI are 1.93% and 0.56%, respectively. If the harmonic components of the DBI and the MDBI are similar and the output capacitor is identical, C_o=60iF,and the capacity of output filter inductor for the DBI and the MDBI

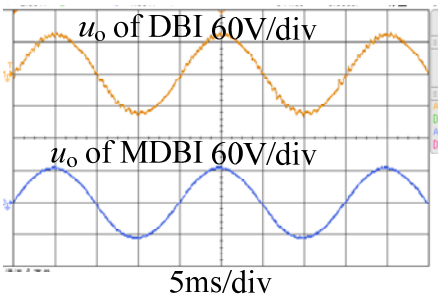

(a) Output voltage of the DBI and the MDBI.

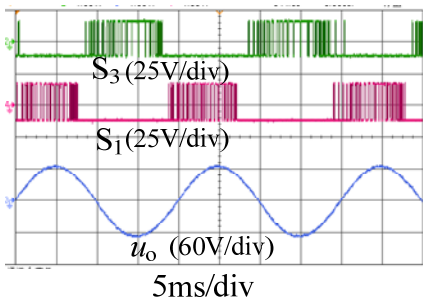

(b) Driving signal of S_3 and S_1 and output voltage u_o.

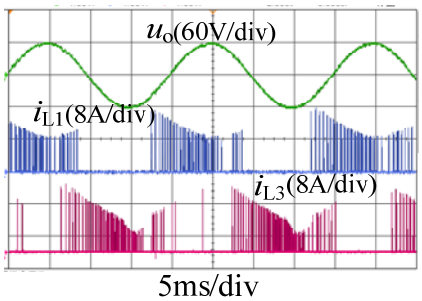

(c) Inductor current i_{L1} and i_{L3} and output voltage u_o.

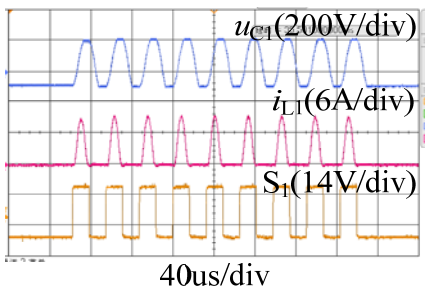

(d)Voltage across C_1, u_{C1}, inductor current L_2, i_{L2}, and the driving signal of S_1.

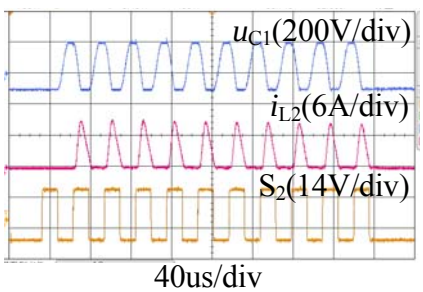

(e) Voltage across C_1, u_{C1}, inductor current L_2, i_{L2}, and the driving signal of S_2.

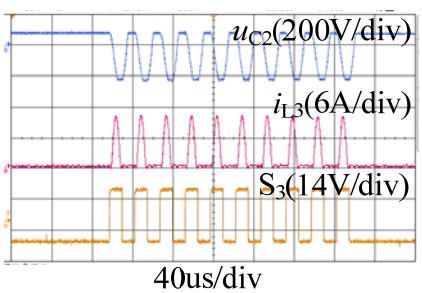

(f) Voltage across C_2, u_{C2}, inductor current L_3, i_{L3}, and the driving signal of S_3.

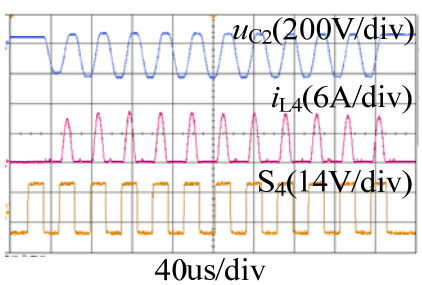

(g) Voltage across C_2, u_{C2}, inductor current L_4, i_{L4}, and the driving signal of S_4.

Fig. 5. Experiment results of the MDBI.

are L_2=L_4=450μH and L_2=L_4=40μH, respectively. The driving signal of S_3 and S_1, and output voltage u_o are shown from top to bottom in Fig. 5(b). The current flowing through inductors L_1 and L_3, i.e., i_{L1} and i_{L3}, and output voltage u_o are illustrated in Fig. 5(c).As shown in Figs. 5(b) and 5(c),output voltage u_o is almost identical with sinusoidal. In the positive half cycle of the output voltage, the working time of the positive soft-switching resonant circuit is longer than that of the negative soft-switching resonant circuit. In the negative half cycle of the output voltage, the working time of the negative soft-switching resonant circuit is longer than the positive soft-switching resonant circuit. The waveforms of the voltage across resonant capacitor C_1, u_{C1}, current flowing through inductor L_1, i_{L1}, and the driving signal of S_1 during a comparison process are depicted in Fig. 5(d). Switch S_1 is turned on and off with ZCS. The voltage across resonant capacitor C_1, u_{C1}, current flowing

through inductor L_2, i_{L2}, and the driving signal of S_2 during a comparison process are shown from top to bottom in Fig. 5(e). Switch S_2 works in ZCS. The voltage across resonant capacitor C_2, u_{C2}, current flowing through inductor L_3, i_{L3}, and the driving signal of S_3 during a comparison process are depicted in Fig. 5(f). Switch S_3 is turned on and off with ZCS. The waveforms of the voltage across resonant capacitor C_2, u_{C2}, current flowing through inductor L_4, i_{L4}, and the driving signal of S_4 during a comparison process are shown in Fig. 5(g). Switch S_4 works in ZCS. As illustrated in Figs. 5(d)-(g), the MDBI works in PDM mode, and the maximum voltage across the resonant capacitor is close to $2U_d$. A very good agreement is shown between the simulation and the experiment results.

VI. CONCLUSION

In this paper, an MBDI has been proposed. A detailed analysis of the topology and working principle of MDBI was performed. The three-level hysteresis controller with the PDM was used to obtain constant switching frequency, which reduced the dimensions of the MDBI and decreased the capacity of the filter inductor. Because of the quasi-resonant link, the MDBI can achieve ZCS at turn on and soft turnoff and decrease the harmonic components with low output voltage. The parameter selection principle of the MDBI was introduced, and the parameter used was given. The mathematical model of the MDBI using symbolic analysis and discrete mapping modeling has been presented. The mathematical model was verified by the simulation results. An experiment prototype was set up, and the experiment results were given. The simulation and experiment results validated the feasibility and correctness of the scheme.

ACKNOWLEDGMENT

This work was supported by Science and Technology Development Program of Shandong Province (No.2013 GSF11607) and the Fundamental Research Funds for the Central Universities of China (No.13CX06090A).

REFERENCES

[1] S. Kwak and J. C. Park, "Switching strategy based on model predictive control of VSI to obtain high efficiency and balanced loss distribution," *IEEE Trans. Power Electron.*, Vol. 29, No. 9, pp. 4551-4557, Nov. 2013.

[2] J. W. Choi and S. K. Sul, "A new compensation strategy reducing voltage/current distortion in PWM VSI systems operating with low output voltages," *IEEE Trans. Ind. Appl.*,Vol. 31, No. 5, pp. 1001-1008, Sep. 1995.

[3] D. Lee, H. Kim, and J. Ahn, "A simple and direct dead-time effect compensation scheme in PWM-VSI," *IEEE Trans. Ind. Appl.*, Vol. 50, No. 5, pp. 3017-3025, Sep. 2014.

[4] D. Leggate and R. J. Kerkman, "Pulse based dead time compensator for PWM voltage inverters," in *Proceeding of IEEE IECON*, pp. 474-481, 1995.

[5] M. R. Islam, Y. Guo, and Z. W. Lin, "An amorphous alloy core medium frequency magnetic-link for medium voltage photovoltaic inverters," *Journal of Applied Physics*, Vol. 115, No. 17, 17E710, Feb. 2014.

[6] X. Huang, H. Yu, J. S. Lai, A. R. Hefner, D. W. Berning, "Characterization of paralleled super junction MOSFET devices under hard and soft-switching conditions," in *Annual of IEEE PESC*, pp. 2145-2150,2001.

[7] G.R. Stanley and K. M. Bradshaw, "Precision DC-to-AC power conversion by optimization of the output current waveform: The half bridge revisited," *IEEE Trans. Power Electron.*, Vol. 14, No. 2, pp. 372-380, Mar. 1999.

[8] J. Liu and Y. G.Y an, "A novel hysteresis current controlled dual buck half bridge inverter," in *Annual of IEEE PESC*, pp. 1615-1620, 2003.

[9] Z. Yao, L. Xiao, and Y. G. Yan, "Dual-buck full-bridge inverter with hysteresis current control," *IEEE Trans. Ind. Electron.*, Vol. 56, No. 8, pp. 3153-3160, Aug. 2009.

[10] Z. Yao, L. Xiao, and Y. G. Yan, "Control strategy for series and parallel output dual-buck half bridge inverters based on DSP control," *IEEE Trans. Power Electron.*, Vol. 24, No. 2, pp. 434-444, Feb. 2009.

[11] P.S. Kumar, N. Vishwanathan, and B. K. Murthy, "Buck-boost interleaved inverter configuration for multiple-load induction cooking application," *Journal of Electrical Engineering & Technology*, Vol. 10, No. 1, pp. 271-279, Jan. 2015.

[12] H. L. Do, "Single-switch buck converter with a ripple-free inductor current," *Journal of Power Electronics*, Vol. 11, No. 4, pp. 507-511, Jul. 2011.

[13] B.R. Lin and W. J. Lin, "Single-switch buck converter with a ripple-free inductor current," *Journal of Power Electronics*, Vol. 11, No. 4, pp. 882-889,Jul. 2011.

[14] P. Sun, C. Liu, and J. S. Lai, "Cascade dual buck inverter with phase-shift control," *IEEE Trans. Power Electron.*, Vol. 27, No. 4, pp. 2067-2077, Apr. 2012.

[15] J. H. Wang, F. H. Zhang, and C. Y. Gong, "Modeling and analysis of inverter with hysteretic current control," *Transactions of China Electrotechnical Society*, Vol. 25, No. 6, pp. 63-69, Jun. 2010.

[16] R. Chen and J. S. Zhang, "Analysis and design of a new topology of soft-switching inverters," *Journal of Power Electronics*, Vol. 13, No. 1, pp. 51-58, Jan. 2013.

[17] Y. F. Chen, S. S. Qiu, and G. Z. Zhang, "Full-order nonlinear modeling and symbolic analysis of frequency modulation quasi-resonant switching converters," *Transactions of China Electrotechnical Society*, Vol. 18, No. 4, pp. 30-34, Apr. 2003.

[18] Y. Sun, L. Li, X. Dai. Y. G. Su, and Z. H. Wang, "Discrete mapping and simulation of a full bridge current-fed soft-switching converter," *Transactions of China Electrotechnical Society*, Vol. 20, No. 6, pp. 20-24, Jun. 2005.

Rong Chen was born in Shandong, China, in 1976. He received his B.S. degree in industrial automation in 1998 and his M.S. degree in control theory and control engineering in 2001 from Shandong University of Science and Technology, Shandong, China. He is currently working toward his Ph.D. degree in control theory and control engineering at China University of Petroleum (Huadong), Qingdao, China. His research interests include electric machine drives, power electronics, high-frequency soft switching converters, and power factor correction.

Jia-Sheng Zhang was born in Shandong, China in 1957. He received his B.S. degree in applied electronic technology from China University of Petroleum, Shandong, China, in 1982 and his M.S. and Ph.D. degrees in electrical and electronic engineering from Beijing Jiaotong University, Beijing, China in 1988 and 1998, respectively. In 1982, he joined the Department of Electrical Engineering, China University of Petroleum, where he is currently employed as a full-time professor. His research interests include power electronics, motor drives, power quality control, renewable distributed power sources, and digital-signal-processor-based control of power converters.

Wei Liu was born in Hebei, China, in 1990. In 2014, he received the M.S. in electrical engineering and automation from China University of Petroleum, Shandong, China, where he is currently working toward his M.S degree in electrical engineering. His research interests include high-frequency DC–AC inverters, soft switching techniques, inverter modeling, and nonlinear control techniques.